Available online at www.sciencedirect.com
SCIENCE DIRECT®

Thermochimica Acta 445 (2006) 49–52

thermochimica acta

www.elsevier.com/locate/tca

High-temperature heat capacities of $EuPO_4$ and $SmPO_4$ synthetic monazites

K. Popa [1], R.J.M. Konings *

European Commission, Joint Research Centre, Institute for Transuranium Elements, P.O. Box 2340, 76125 Karlsruhe, Germany

Received 26 January 2006; received in revised form 23 March 2006; accepted 28 March 2006
Available online 7 April 2006

Abstract

High-temperature enthalpy increments of monazite-type $EuPO_4$ and $SmPO_4$ were measured by drop calorimetry in the temperature range 450–1570 K and the heat capacity was derived. The excess heat capacity C_{exs} was calculated by subtracting the lattice heat capacity, interpolated from isostructural $LaPO_4$ ($4f^0$) and $GdPO_4$ ($4f^7$) compounds. A good agreement was found with C_{exs} calculated from (estimated) crystal field energies. The heat capacity of $PrPO_4$ was estimated with this approach.

Keywords: Drop calorimetry; High-temperature heat capacity; Enthalpy; Lanthanide phosphates

1. Introduction

The large amounts of high-level nuclear waste accumulated in the world after 1945 (e.g., more than 1400 metric tonnes plutonium [1]) have stimulated many researchers to study solutions for its safe immobilization. Monazite, the idealised formula of which is $LnPO_4$ (Ln = La to Gd), has been proposed as a ceramic immobilization matrix for separated plutonium and minor actinides, due to various favourable chemical and physical characteristics, such as radiation resistance, aqueous durability and mechanical durability [2]. The actinide loading of monazite-type ceramics can be high and can contain mixed valence states, since the ternary An(III) orthophosphates $PuPO_4$, $AmPO_4$ and $CmPO_4$ but also some quaternary An(IV) phosphates, for instance $CaU(PO_4)_2$ [3] and $M^{II}Th(PO_4)_2$ (M^{II} = Ca, Sr, Ba, Cd, Pb) [4], all have the monazite structure ($P2_1/n$ space group) and are expected to show significant mutual solubility in the solid state.

Apart from the nuclear applications, monazites are considered as interesting high-temperature ceramics and could find application in the disposal of non-radioactive hazardous waste, in transportation technology, as luminescent materials, scintillators or catalysts [5].

In spite of the wide field of applications, there is a lack of knowledge of the thermodynamic properties of the monazite end-members at high temperatures. This was the incentive for our systematic study on the heat capacity of relevant lanthanide and actinide orthophophates and in previous papers we have reported results for $LnPO_4$ (Ln = La, Ce, Nd and Gd) in the temperature range (0.5–1570 K) [6–10] as well as of $PuPO_4$ and $(La_{0.9}Pu_{0.1})PO_4$ in the temperature range 5–300 K [11,12]. The results for these isostructural $LnPO_4$ compounds showed that the heat capacity could be described satisfactorily as the sum of a lattice contribution interpolated from $LaPO_4$ ($4f^0$) and $GdPO_4$ ($4f^7$) compounds, and an excess contribution arising from 4f electron excitation, calculated from crystal field energies.

The present paper reports enthalpy increment measurements for $EuPO_4$ and $SmPO_4$ by drop calorimetry in the temperature range 450–1570 K, from which we derive the high-temperature heat capacity data. The results are used for an additional test of the heat capacity description.

2. Experimental

The $EuPO_4$ and $SmPO_4$ powders were synthesised by sol–gel reaction starting from Eu_2O_3 (Merck, 99.99%) and Sm_2O_3

---

* Corresponding author. Tel.: +49 72 47 951 391; fax: +49 72 47 591 566.
E-mail address: rudy.konings@cec.eu.int (R.J.M. Konings).

[1] Permanent address: “Al.I. Cuza” University, Department of Inorganic and Analytical Chemistry, 11 – Carol I Blvd., 700506 Iasi, Romania.

0040-6031/$ – see front matter © 2006 Elsevier B.V. All rights reserved.
doi:10.1016/j.tca.2006.03.023

Table 1
The crystal data of $EuPO_4$ and $SmPO_4$ monazites

a (nm)	b (nm)	c (nm)	β (°)	V (nm^3)	Reference
$EuPO_4$					
0.66226(9)[a]	0.68188(2)	0.63391(9)	103.969(1)	0.2778(2)	Present work
0.66390	0.68230	0.63180	104.000	0.2777[b]	Mulica et al. [13]
0.66131	0.68189	0.63491	103.961	0.2778[b]	Ni et al. [14]
0.66660	0.68684	0.63486	103.910	0.2821[b]	Ushakov et al. [15]
$SmPO_4$					
0.66902(9)	0.68935(5)	0.63714(3)	103.871(9)	0.2853	Present work
0.66690	0.68680	0.63510	103.920	0.2824[b]	Mulica et al. [13]
0.66181	0.68877	0.63653	103.861	0.2817[b]	Ni et al. [14]
0.66891	0.68958	0.63770	103.910	0.2855[b]	Ushakov et al. [15]

[a] The number in parenthesis are uncertainty in last digit (e.s.d. from least squares analysis).
[b] Calculated from the lattice parameters.

(Elcomat Lmf, 99.99%). The oxides were dissolved in the equimolar amount of 63% HNO_3 and reacted with 85% H_3PO_4 (10% excess). By adding 5 mol dm^{-3} NH_4OH to the solution to give pH 4, the formation of gels was initiated. These gels were filtered (Robu-Glass filtering crucible, porosity 5) and washed with distilled water. The precipitates were heated in alumina crucibles at 1473 K for 24 h (with heating and cooling ramp of 200 K h^{-1}).

The powders thus obtained were ground in an agate mortar, analysed by powder X-ray diffraction (XRD) at room temperature for phase purity (Bruker D8 diffractometer, Cu Kα), then manually pressed into pellets (d = 7 mm, h = 4–5 mm) and sintered at T = 1873 K during 5 h (with heating and cooling ramp of 300 K h^{-1}). After this procedure, the purity of the sintered samples was verified again by XRD analysis. A single phase with monoclinic monazite structure ($P2_1/n$ space group) was observed. The lattice parameters of the compounds are presented in Table 1. Unit cell parameters were refined on powdered samples by a Rietveld-type method using the Fullprof software. These data are in good agreement with data reported earlier [13–15]. We also performed DTA/TG measurements (Netsch STA 449C Jupiter, in alumina crucibles in an air atmosphere) on the obtained compounds, showing no thermal effects up to 1873 K.

The enthalpy increments from room temperature to the respective temperature of a given run were determined with a Setaram multi-detector high-temperature calorimeter (MHTC-96) operating in a drop mode. Platinum metal rods (99.95% purity) were used as reference material; the samples (with masses of 70–90 mg) and the reference (with masses of 300–330 mg) were ordered alternatively in the feeding chamber and equilibrated at ambient temperature. The details of our equipment and the temperature calibration were previously described by Sedmidubský et al. [16]. All evaluations of background subtraction and peak integration were done by DSCEval software [17].

3. Results

The experimental results for the enthalpy increments of $EuPO_4$ and $SmPO_4$ monazites are presented in Table 2 and are shown in Figs. 1 and 2 as plots of the reduced enthalpy increment $\{H^\circ(T) - H^\circ(298.15\,\mathrm{K})\}/(T - 298.15)$ as a function of temperature. The error bar is calculated as the standard deviation of four independent measurements.

The enthalpy increments for $EuPO_4$ have been fitted to the Maier-Kelly type polynomial equation that was also used in our previous studies of $LaPO_4$, $CePO_4$, $NdPO_4$ and $GdPO_4$. This

Table 2
Enthalpy increment $H(T_m) - H(T_a)$ of the $EuPO_4$ and $SmPO_4$ monazites; T_m, measured temperature; T_a, ambient temperature

$EuPO_4$			$SmPO_4$		
T_m (K)	T_a (K)	$H(T_m) - H(T_a)$ (J mol^{-1})	T_m (K)	T_a (K)	$H(T_m) - H(T_a)$ (J mol^{-1})
483.9	296.5	23417 ± 632	484.0	297.2	21346 ± 853
587.0	300.6	37966 ± 1843	586.4	297.8	36396 ± 1088
687.2	298.4	51879 ± 1357	688.2	298.5	50515 ± 1722
787.2	295.9	66059 ± 1400	787.4	298.6	65520 ± 1009
887.2	296.4	81410 ± 1514	887.2	299.7	81265 ± 2056
986.7	296.3	96061 ± 1008	986.8	299.2	95730 ± 2776
1085.9	297.5	110579 ± 2731	1086.2	300.0	109171 ± 775
1185.9	299.9	126695 ± 2242	1186.0	300.1	124573 ± 1881
1285.8	300.5	142912 ± 3173	1294.5	300.1	142314 ± 3187
1385.7	300.3	160831 ± 4181	1385.4	301.6	160389 ± 1491
1486.3	300.4	173332 ± 2692	1485.8	301.4	177679 ± 6769
1566.3	300.7	188025 ± 3309	1557.0	302.6	188152 ± 3556
			1566.4	301.3	185390 ± 3170

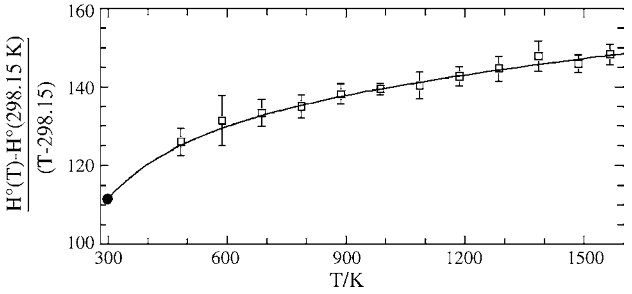

Fig. 1. Plot of the reduced enthalpy increment of $EuPO_4$; (□) experimental results; (●) calculated value at $T = 298.15$ K.

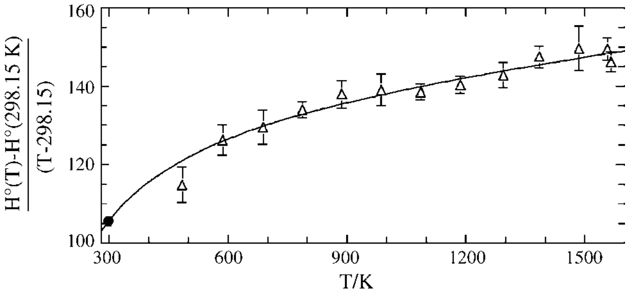

Fig. 2. Plot of the reduced enthalpy increment of $SmPO_4$; (△) experimental results; (●) calculated value at $T = 298.15$ K.

equation was found to give a satisfactory fit of our results, and permits a reliable extrapolation to higher temperatures. By differentiation we obtain for the heat capacity of $EuPO_4$:

$$C_p^{\circ}(\mathrm{J\,K^{-1}\,mol^{-1}}) = 137.5600 + 17.6934 \times 10^{-3}(T(\mathrm{K})) - 2.7854 \times 10^{6}(T(\mathrm{K}))^{-2} \quad (1)$$

This equation was constrained to $C_p^{\circ}(298.15\,\mathrm{K}) = 111.5\,\mathrm{J\,K^{-1}\,mol^{-1}}$ which was estimated as the sum of the lattice heat capacity series interpolated in the lanthanide monazite series between the values for $LaPO_4$ and $GdPO_4$, and the excess heat capacity at $T = 298.15$ K calculated from the crystal field energies. Table 3 shows the validity and reliability of this approach, as the agreement between the calculated and experimental values for $CePO_4$ and $NdPO_4$ is excellent.

Table 3
The calculated and the measured heat capacity ($\mathrm{J\,K^{-1}\,mol^{-1}}$) at $T = 298.15$ K for the lanthanides orthophosphates series

	C_{lat}	C_{ele}	$C_{calc} = C_{lat} + C_{ele}$	C_{exp}	$C_{exp} - C_{calc}$
$LaPO_4$	101.28	0.00	101.28	101.28	0.00
$CePO_4$	101.41[a]	5.22	106.63	106.40[b]	−0.23
$PrPO_4$	101.55[a]	4.49	106.04		
$NdPO_4$	101.68[a]	3.24	104.92	104.80[c]	−0.12
$SmPO_4$	101.94[a]	3.65	105.59		
$EuPO_4$	102.08[a]	9.41	111.49		
$GdPO_4$	102.21	0.00	102.21	102.21	0.00

[a] Calculated from the heat capacity of $LaPO_4$ and $GdPO_4$.
[b] Value from ref. [9].
[c] Value from ref. [10].

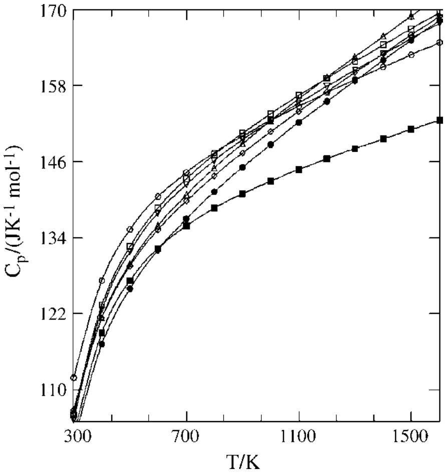

Fig. 3. Plot of the heat capacity of the lanthanide monazite-type orthophosphates; $LaPO_4$ (●), $CePO_4$ (◊), $NdPO_4$ (△), $PrPO_4$ (▽), $EuPO_4$ (□), $SmPO_4$ (○) and $GdPO_4$ (■) against temperature.

Similarly, the following heat capacity equation was obtained by fitting the enthalpy data for $SmPO_4$:

$$C_p^{\circ}(\mathrm{J\,K^{-1}\,mol^{-1}}) = 133.1252 + 23.4677 \times 10^{-3}(T(\mathrm{K})) - 3.06879 \times 10^{6}(T(\mathrm{K}))^{-2} \quad (2)$$

This equation was constrained to $C_p^{\circ}(298.15\,\mathrm{K}) = 105.6\,\mathrm{J\,K^{-1}\,mol^{-1}}$, estimated in a similar manner as for $EuPO_4$ (Table 3).

4. Discussion

The derived heat capacity curves for the $LnPO_4$ series are plotted in Fig. 3 as a function of temperature. The curves are very close except for that of $GdPO_4$, which is significantly lower in the high-temperature range. As discussed in earlier papers [9,10], the total heat capacity of these compounds is the sum of a lattice component, resulting principally from the lattice vibrations, and an excess or electronic term, resulting from thermal excitation of the f-electrons:

$$C_p = C_{lat} + C_{exs} \quad (3)$$

Since no electronic excess contribution is present in $LaPO_4$ ($4f^0$) and $GdPO_4$ ($4f^7$), due to the empty and half-filled 4f electron shell configurations, their curves represent the lattice heat capacity. C_{lat} decreases linearly between these two compounds, but since the excess heat capacity in the 4f lanthanide ions with incompletely filled electron shell configurations is significant and increases along the series, the other curves group around that of $LaPO_4$.

Fig. 4 shows the excess heat capacity (C_{exs}) of $EuPO_4$ and $SmPO_4$, calculated from the present experimental results by subtracting the lattice contribution (C_{lat}) interpolated from the equations for $LaPO_4$ and $GdPO_4$. The results for C_{exs} thus obtained can be compared to the excess heat capacity calculated from crystal field energies for $EuPO_4$ and $SmPO_4$. For $EuPO_4$, we included the energies of the $^7F_0$ to $^7F_4$ states, for $SmPO_4$ the $^6H_{5/2}$ to $^6F_{11/2}$ states. The energies of the lowest

Table 4
The polynomial coefficients of the heat-capacity and the thermodynamic functions of formation of the $LnPO_4$ monazites

	a	$b \times 10^3$	$c \times 10^{-6}$	$\Delta_f H^\circ$ (298.15 K)[b] (kJ mol^{-1})	S° (298.15 K) (J K^{-1} mol^{-1})	$\Delta_f G^\circ$ (298.15 K) (kJ mol^{-1})
$LaPO_4$	121.1275 ± 7.899	30.1156 ± 9.394	−2.5625 ± 0.4571	−1969.7 ± 1.9	108.28[c]	−1850.5 ± 1.9
$CePO_4$	125.2087 ± 5.415	27.8936 ± 7.100	−2.4085 ± 0.3001	−1969.5 ± 2.2	119.97[d]	−1849.9 ± 2.3
$PrPO_4$	124.4998[a]	30.3743[a]	−2.4495[a]	−1961.8 ± 3.1	123.2[e]	−1841.9 ± 3.3
$NdPO_4$	132.9631 ± 7.577	22.5413 ± 8.346	−3.1009 ± 0.4573	−1967.9 ± 2.5	122.9[f]	−1848.4 ± 2.6
$SmPO_4$	133.1252 ± 11.465	23.4677 ± 13.203	−3.0687 ± 0.7161	−1965.8 ± 2.9	122.5[e]	−1847.0 ± 3.0
$EuPO_4$	137.5600 ± 10.465	17.6934 ± 9.417	−2.7854 ± 1.2008	−1864.4 ± 2.7	117.2[e]	−1741.6 ± 2.8
$GdPO_4$	133.2371 ± 8.822	12.7933 ± 10.789	−3.0972 ± 0.5074	−1958.5 ± 2.2	124.57[c]	−1840.8 ± 2.3

[a] Estimated values.
[b] Recalculated from the experimental results of Ushakov et al. [15] using the recent assessed values for the enthalpies of formation of the lanthanide oxides [19].
[c] Thiriet et al. [7].
[d] Thiriet et al. [6].
[e] Estimated [7].
[f] Popa et al. [10].

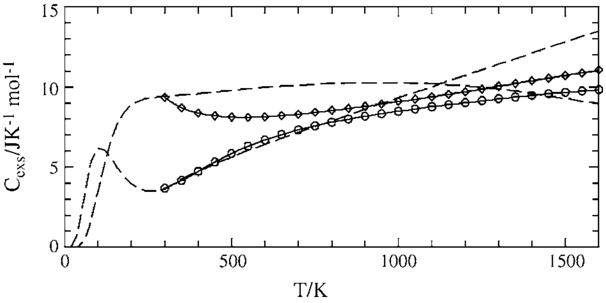

Fig. 4. Plot of the excess heat capacity of $EuPO_4$ (◇) and $SmPO_4$ (○) against temperature; the symbols show the experimental results, the broken lines the calculated results.

states are the values calculated by Thiriet et al. [7], all other values are estimates based on the energy levels in various hosts [18]. The agreement between ‘experimental’ and calculated values is acceptable for both $EuPO_4$ and $SmPO_4$, considering that C_{lat} is the difference of two numbers that are a factor 10^2 larger. It should also be realised that the equations were constrained to the calculated values at $T = 298.15$ K.

In view of the good agreement for $SmPO_4$ and $EuPO_4$ found here, consistent with the results for $CePO_4$ and $NdPO_4$ reported earlier [9,10], we can predict the heat capacity of the remaining lanthanide monazite compound $PrPO_4$ using the same approach. The resulting heat capacity equation is listed in Table 4. Included in this table are the results for the high-temperature heat capacity for all the $LnPO_4$ monazite compounds that we studied (Ln = La, Ce, Nd, Sm, Eu, Gd). The coefficients a, b and c refer to the standard Maier-Kelley polynomial equation:

$$C^\circ_p(\mathrm{J\,mol^{-1}\,K^{-1}}) = a + b \times 10^{-3}(T(\mathrm{K})) + c \times 10^{6}(T(\mathrm{K}))^{-2} \tag{4}$$

Also included in this table are the values for the enthalpy of formation, entropy and Gibbs energy of formation at $T = 298.15$ K.

Further improvement of the description of the results in terms of lattice and excess heat capacity contributions could come from accurate determination of the crystal field energies of these compounds.

Acknowledgements

The authors thank Mr. Daniel Bouëxière for the X-ray characterisation of the samples. K.P. acknowledges the European Commission for support given in the frame of the program “Training and Mobility of Researchers”.

References

[1] R.C. Ewing, W.J. Weber, J. Lian, J. Appl. Phys. 95 (2004) 5949–5971.
[2] L.A. Boatner, M.M. Abraham, B.C. Sales, Inorg. Chim. Acta 94 (1984) 146–149.
[3] R. Podor, M. Cuney, N. Nguyen Trung, Am. Mineral. 80 (1995) 1261–1268.
[4] J.-M. Montel, J.-L. Devidal, D. Avignant, Chem. Geol. 191 (2002) 89–104.
[5] L.A. Boatner, Phosphates: geochemical, geobiological and materials importance, in: P.H. Ribbe, J.J. Rosso (Eds.), Reviews in Mineralogy and Geochemistry, Mineralogical Society of America/Geochemical Society, 2002, pp. 87–121 (Chapter 4).
[6] C. Thiriet, R.J.M. Konings, P. Javorský, F. Wastin, Phys. Chem. Miner. 31 (2005) 347–352.
[7] C. Thiriet, R.J.M. Konings, P. Javorský, N. Magnani, F. Wastin, J. Chem. Thermodyn. 37 (2005) 129–137.
[8] C. Thiriet, R.J.M. Konings, P. Javorský, Solid State Commun. 134 (2005) 409–412.
[9] K. Popa, D. Sedmidubský, O. Beneš, C. Thiriet, R.J.M. Konings, J. Chem. Thermodyn. (2006) (online first, doi:10.1016/j.jct.2005.08.019).
[10] K. Popa, F. Jutier, F. Wastin, R.J.M. Konings, J. Chem. Thermodyn. (2006) (online first, doi:10.1016/j.jct.2006.02.006).
[11] C. Thiriet, R.J.M. Konings, F. Wastin, J. Nucl. Mater. 344 (2005) 56–60.
[12] K. Popa, E. Colineau, F. Wastin, R.J.M. Konings, in preparation.
[13] D.F. Mulica, D.A. Grossie, L.A. Boatner, Inorg. Chim. Acta 109 (1985) 105–110.
[14] Y. Ni, J.M. Hughes, A.N. Mariano, Am. Mineral. 80 (1995) 21–26.
[15] S.V. Ushakov, K.B. Helean, A. Navrotsky, L.A. Boatner, J. Mater. Res. 16 (2001) 2623–2632.
[16] D. Sedmidubský, O. Beneš, R.J.M. Konings, J. Chem. Thermodyn. 37 (2005) 1098–1103.
[17] D. Sedmidubský, DSCEval—Software for DSC-data evaluation, Institute of Chemical Technology, Prague, Czech Republic.
[18] C.A. Morrison, R.P. Leavit, in: K.A. Gschneidner Jr., L. Eyring (Eds.), Handbook on the Physics and Chemistry of Rare Earths, vol. 5, 1982, p. 461 (Chapter 46).
[19] L.R. Morss, R.J.M. Konings, Thermochemistry of binary rare earth oxides, in: G. Adachi, N. Imanaka, Z. Zhang (Eds.), Binary Rare Earth Oxides, Springer Verlag, 2004, pp. 163–188 (Chapter 7).